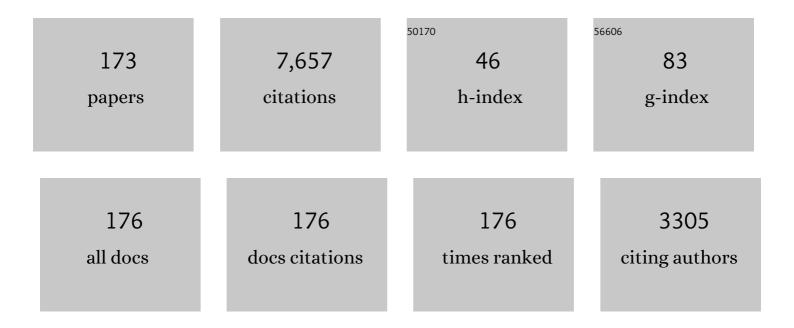
List of Publications by Year in descending order

Source: https://exaly.com/author-pdf/10594645/publications.pdf Version: 2024-02-01



#	Article	IF	CITATIONS
1	Chemical composition dependence of the strength and ductility enhancement by solute hydrogen in Fe–Cr–Ni-based austenitic alloys. Materials Science & Engineering A: Structural Materials: Properties, Microstructure and Processing, 2022, 836, 142681.	2.6	6
2	Hydrogen-accelerated fatigue crack growth of equiatomic Fe–Cr–Ni–Mn–Co high-entropy alloy evaluated by compact tension testing. Materials Science & Engineering A: Structural Materials: Properties, Microstructure and Processing, 2022, 848, 143394.	2.6	5
3	Strain rate and temperature effects on hydrogen embrittlement of stable and metastable high-entropy alloys. , 2022, 25, 5-14.		0
4	Three-dimensional characterization of low-cycle fatigue crack morphology in TRIP-maraging steel: Crack closure, geometrical uncertainty and wear. International Journal of Fatigue, 2021, 143, 106032.	2.8	1
5	Potential Effects of Short-Range Order on Hydrogen Embrittlement of Stable Austenitic Steels—A Review. Advanced Structured Materials, 2021, , 1-18.	0.3	0
6	Fatigue Crack Growth at Different Frequencies and Temperatures in an Fe-based Metastable High-entropy Alloy. ISIJ International, 2021, 61, 641-647.	0.6	7
7	{111} Trace Analysis in ECC Images ―toward <i>In-Situ</i> Observation of Deformation Behavior in FCC Bulk Specimens. Nippon Kinzoku Gakkaishi/Journal of the Japan Institute of Metals, 2021, 85, 17-22.	0.2	0
8	Strain rate and hydrogen effects on crack growth from a notch in a Fe-high-Mn steel containing 1.1Âwt% solute carbon. International Journal of Hydrogen Energy, 2020, 45, 1125-1139.	3.8	19
9	Hydrogen, as an alloying element, enables a greater strength-ductility balance in an Fe-Cr-Ni-based, stable austenitic stainless steel. Acta Materialia, 2020, 199, 181-192.	3.8	44
10	Effects of Mn Content and Grain Size on Hydrogen Embrittlement Susceptibility of Face-Centered Cubic High-Entropy Alloys. Metallurgical and Materials Transactions A: Physical Metallurgy and Materials Science, 2020, 51, 5612-5616.	1.1	30
11	Recent Studies on the Nature and State of Carbon Atoms in Iron. Tetsu-To-Hagane/Journal of the Iron and Steel Institute of Japan, 2020, 106, 331-341.	0.1	1
12	Hydrogen Enhances Shape Memory Effect of a Ferrous Face-Centered Cubic Alloy. Metallurgical and Materials Transactions A: Physical Metallurgy and Materials Science, 2020, 51, 4439-4441.	1.1	6
13	In-Situ Electron Channeling Contrast Imaging under Tensile Loading: Residual Stress, Dislocation Motion, and Slip Line Formation. Scientific Reports, 2020, 10, 2622.	1.6	10
14	Growth Behavior of a Mechanically Long Fatigue Crack in an FeCrNiMnCo High Entropy Alloy: A Comparison with an Austenitic Stainless Steel. ISIJ International, 2020, 60, 175-181.	0.6	13
15	Fatigue Behavior in an Fe-N Binary Ferritic Steel: Similarity and Difference between Carbon and Nitrogen. Tetsu-To-Hagane/Journal of the Iron and Steel Institute of Japan, 2020, 106, 413-419.	0.1	2
16	Effect of Hydrogen on the Substructure of Lenticular Martensite in Fe-31Ni Alloy. Metallurgical and Materials Transactions A: Physical Metallurgy and Materials Science, 2019, 50, 4027-4036.	1.1	7
17	Detection of hydrogen effusion before, during, and after martensitic transformation: Example of multiphase transformation-induced plasticity steel. International Journal of Hydrogen Energy, 2019, 44, 26028-26035.	3.8	12
18	EBSD and ECCI Based Assessments of Inhomogeneous Plastic Strain Evolution Coupled with Digital Image Correlation. Tetsu-To-Hagane/Journal of the Iron and Steel Institute of Japan, 2019, 105, 222-230.	0.1	10

#	Article	IF	CITATIONS
19	Fatigue Behavior in an Fe–N Binary Ferritic Steel: Similarity and Difference between Carbon and Nitrogen. ISIJ International, 2019, 59, 186-191.	0.6	3
20	Grain refinement effect on hydrogen embrittlement resistance of an equiatomic CoCrFeMnNi high-entropy alloy. International Journal of Hydrogen Energy, 2019, 44, 17163-17167.	3.8	51
21	Evolution of Quasi-Brittle Hydrogen-Assisted Damages in a Dual-Phase Steel. Nippon Kinzoku Gakkaishi/Journal of the Japan Institute of Metals, 2019, 83, 221-230.	0.2	2
22	Revisiting the effects of hydrogen on deformation-induced Î ³ -ε martensitic transformation. Materials Letters, 2019, 249, 197-200.	1.3	22
23	Overview of metastability and compositional complexity effects for hydrogen-resistant iron alloys: Inverse austenite stability effects. Engineering Fracture Mechanics, 2019, 214, 123-133.	2.0	33
24	Growth Behavior of a Mechanically Long Fatigue Crack in an FeCrNiMnCo High Entropy Alloy: A Comparison with an Austenitic Stainless Steel. Tetsu-To-Hagane/Journal of the Iron and Steel Institute of Japan, 2019, 105, 215-221.	0.1	7
25	Fatigue Crack Propagation Resistance in Metastable Laminated Microstructures. Materia Japan, 2019, 58, 206-213.	0.1	Ο
26	EBSD- and ECCI-based Assessments of Inhomogeneous Plastic Strain Evolution Coupled with Digital Image Correlation. ISIJ International, 2019, 59, 2334-2342.	0.6	14
27	Lowering Strain Rate Simultaneously Enhances Carbon- and Hydrogen-Induced Mechanical Degradation in an Fe-33Mn-1.1C Steel. Metallurgical and Materials Transactions A: Physical Metallurgy and Materials Science, 2019, 50, 1137-1141.	1.1	12
28	Evolution of Quasi-Brittle Hydrogen-Assisted Damages in a Dual-Phase Steel. Materials Transactions, 2019, 60, 2368-2377.	0.4	7
29	Characteristics of plastic deformation associated with hydrogen-induced delayed crack propagation in a sheet of single-crystal Fe-Si alloy. The Proceedings of the Materials and Mechanics Conference, 2019, 2019, OS0111.	0.0	Ο
30	High-concentration carbon assists plasticity-driven hydrogen embrittlement in a Fe-high Mn steel with a relatively high stacking fault energy. Materials Science & Engineering A: Structural Materials: Properties, Microstructure and Processing, 2018, 717, 78-84.	2.6	18
31	Non-propagating fatigue cracks in austenitic steels with a micro-notch: Effects of dynamic strain aging, martensitic transformation, and microstructural hardness heterogeneity. International Journal of Fatigue, 2018, 113, 359-366.	2.8	12
32	Comparative study of hydrogen embrittlement in stable and metastable high-entropy alloys. Scripta Materialia, 2018, 150, 74-77.	2.6	84
33	Hydrogen trapping in carbon supersaturated αâ€'iron and its decohesion effect in martensitic steel. Scripta Materialia, 2018, 149, 79-83.	2.6	40
34	Fatigue Behavior of Fe-Cr-Ni-based Metastable Austenitic Steels with an Identical Tensile Strength and Different Solute Carbon Contents. ISIJ International, 2018, 58, 1910-1919.	0.6	5
35	Fatigue Behavior of Fe-Cr-Ni-based Metastable Austenitic Steels with an Identical Tensile Strength and Different Solute Carbon Contents. Tetsu-To-Hagane/Journal of the Iron and Steel Institute of Japan, 2018, 104, 88-97.	0.1	1
36	Localized Plasticity and Associated Cracking in Stable and Metastable High-Entropy Alloys Pre-Charged with Hydrogen. Procedia Structural Integrity, 2018, 13, 716-721.	0.3	12

#	Article	IF	CITATIONS
37	Strain Rate Sensitivity of Microstructural Damage Evolution in a Dual-Phase Steel Pre-Charged with Hydrogen. Procedia Structural Integrity, 2018, 13, 710-715.	0.3	4
38	Overview of Dynamic Strain Aging and Associated Phenomena in Fe–Mn–C Austenitic Steels. ISIJ International, 2018, 58, 1383-1395.	0.6	47
39	Randomization of Ferrite/austenite Orientation Relationship and Resultant Hardness Increment by Nitrogen Addition in Vanadium-microalloyed Low Carbon Steels Strengthened by Interphase Precipitation. ISIJ International, 2018, 58, 542-550.	0.6	13
40	An unconventional hydrogen effect that suppresses thermal formation of the hcp phase in fcc steels. Scientific Reports, 2018, 8, 16136.	1.6	15
41	Overview of Dynamic Strain Aging and Associated Phenomena in Fe-Mn-C Austenitic Steels. Tetsu-To-Hagane/Journal of the Iron and Steel Institute of Japan, 2018, 104, 187-200.	0.1	6
42	Optical Microscopy-Based Damage Quantification: an Example of Cryogenic Deformation of a Dual-Phase Steel. ISIJ International, 2018, 58, 179-185.	0.6	12
43	Microstructural damage evolution and arrest in binary Fe–high-Mn alloys with different deformation temperatures. International Journal of Fracture, 2018, 213, 193-206.	1.1	9
44	Surface orientation dependence of hydrogen flux in lenticular martensite of an Fe-Ni-C alloy clarified through in situ silver decoration technique. Materials Letters, 2018, 228, 273-276.	1.3	5
45	Small fatigue crack growth resistance of TRIP-maraging steel. The Proceedings of Conference of Kyushu Branch, 2018, 2018.71, C44.	0.0	0
46	Small crack behavior of extruded Mg-Gd-Y-Zr alloy under high cycle fatigue. The Proceedings of Conference of Kyushu Branch, 2018, 2018.71, C45.	0.0	0
47	Bone-like crack resistance in hierarchical metastable nanolaminate steels. Science, 2017, 355, 1055-1057.	6.0	297
48	Multiscale in situ deformation experiments: A sequential process from strain localization to failure in a laminated Ti-6Al-4V alloy. Materials Characterization, 2017, 128, 217-225.	1.9	14
49	Effects of martensitic transformability and dynamic strain age hardenability on plasticity in metastable austenitic steels containing carbon. Journal of Materials Science, 2017, 52, 7868-7882.	1.7	38
50	Recent progress in microstructural hydrogen mapping in steels: Quantification, kinetic analysis, and multi-scale characterisation. Materials Science and Technology, 2017, 33, 1481-1496.	0.8	125
51	Overview of hydrogen embrittlement in high-Mn steels. International Journal of Hydrogen Energy, 2017, 42, 12706-12723.	3.8	228
52	Hydrogen desorption and cracking associated with martensitic transformation in Fe-Cr-Ni-Based austenitic steels with different carbon contents. International Journal of Hydrogen Energy, 2017, 42, 26423-26435.	3.8	39
53	Room-temperature blue brittleness of Fe-Mn-C austenitic steels. Scripta Materialia, 2017, 141, 20-23.	2.6	37
54	Effects of ε-martensitic transformation on crack tip deformation, plastic damage accumulation, and slip plane cracking associated with low-cycle fatigue crack growth. International Journal of Fatigue, 2017, 103, 533-545.	2.8	27

#	Article	IF	CITATIONS
55	In situ observations of silver-decoration evolution under hydrogen permeation: Effects of grain boundary misorientation on hydrogen flux in pure iron. Scripta Materialia, 2017, 129, 48-51.	2.6	66
56	Comparative study on small fatigue crack propagation between Fe-30Mn-3Si-3Al and Fe-23Mn-0.5C twinning-induced plasticity steels: Aspects of non-propagation of small fatigue cracks. International Journal of Fatigue, 2017, 94, 1-5.	2.8	27
57	Two-dimensional Moiré phase analysis for accurate strain distribution measurement and application in crack prediction. Optics Express, 2017, 25, 13465.	1.7	38
58	Combined Multi-scale Analyses on Strain/Damage/Microstructure in Steel: Example of Damage Evolution Associated with lµ-martensitic Transformation. Tetsu-To-Hagane/Journal of the Iron and Steel Institute of Japan, 2016, 102, 227-236.	0.1	6
59	Effect of Additional Boron Amount on Surface Roughness after Lathe Turning in h-BN Dispersed Type 304 Stainless Steels. ISIJ International, 2016, 56, 1031-1037.	0.6	2
60	On Strengthening of Austenitic Stainless Steel by Large Strain Cold Working. ISIJ International, 2016, 56, 1289-1296.	0.6	30
61	Combined Multi-scale Analyses on Strain/Damage/Microstructure in Steel: Example of Damage Evolution Associated with <i>ε</i> -martensitic Transformation. ISIJ International, 2016, 56, 2037-2046.	0.6	25
62	Design Concept and Applications of Fe–Mn–Si-Based Alloys—from Shape-Memory to Seismic Response Control. Materials Transactions, 2016, 57, 283-293.	0.4	117
63	Martensitic transformation-induced hydrogen desorption characterized by utilizing cryogenic thermal desorption spectroscopy during cooling. Scripta Materialia, 2016, 122, 50-53.	2.6	34
64	In situ microscopic observations of low-cycle fatigue-crack propagation in high-Mn austenitic alloys with deformation-induced Îμ-martensitic transformation. Acta Materialia, 2016, 112, 326-336.	3.8	61
65	Hexagonal close-packed Martensite-related Fatigue Crack Growth under the Influence of Hydrogen: Example of Fe–15Mn–10Cr–8Ni–4Si Austenitic Alloy. Scripta Materialia, 2016, 113, 6-9.	2.6	17
66	Hydrogen Embrittlement Susceptibility of Fe-Mn Binary Alloys with High Mn Content: Effects of Stable and Metastable Îμ-Martensite, and Mn Concentration. Metallurgical and Materials Transactions A: Physical Metallurgy and Materials Science, 2016, 47, 2656-2673.	1.1	67
67	Effect of strain amplitude on the low-cycle fatigue behavior of a new Fe–15Mn–10Cr–8Ni–4Si seismic damping alloy. International Journal of Fatigue, 2016, 88, 132-141.	2.8	54
68	Deformation microstructural evolution and strain hardening of differently oriented grains in twinning-induced plasticity β titanium alloy. Materials Science & Engineering A: Structural Materials: Properties, Microstructure and Processing, 2016, 659, 1-11.	2.6	38
69	Hydrogen-assisted damage in austenite/martensite dual-phase steel. Philosophical Magazine Letters, 2016, 96, 9-18.	0.5	25
70	Delamination toughening assisted by phosphorus in medium-carbon low-alloy steels with ultrafine elongated grain structures. Materials Science & Engineering A: Structural Materials: Properties, Microstructure and Processing, 2016, 649, 135-145.	2.6	27
71	Roles of ε-martensite on Resistance to Crack Growth:. The Proceedings of Mechanical Engineering Congress Japan, 2016, 2016, G0300103.	0.0	0
72	Importance of crack-propagation-induced Îμ-martensite in strain-controlled low-cycle fatigue of high-Mn austenitic steel. Philosophical Magazine Letters, 2015, 95, 303-311.	0.5	25

#	Article	IF	CITATIONS
73	Effects of Si on Tensile Properties Associated with Deformation-Induced ε-Martensitic Transformation in High Mn Austenitic Alloys. Nippon Kinzoku Gakkaishi/Journal of the Japan Institute of Metals, 2015, 79, 657-663.	0.2	3
74	Effects of Si on Tensile Properties Associated with Deformation-Induced ε-Martensitic Transformation in High Mn Austenitic Alloys. Materials Transactions, 2015, 56, 819-825.	0.4	19
75	Deformation Twinning Behavior of Twinning-induced Plasticity Steels with Different Carbon Concentrations – Part 2: Proposal of Dynamic-strain-aging-assisted Deformation Twinning. ISIJ International, 2015, 55, 1754-1761.	0.6	37
76	<i>Îμ</i> → <i>γ</i> Reverse Transformation-induced Hydrogen Desorption and Mn Effect on Hydrogen Uptake in Fe–Mn Binary Alloys. ISIJ International, 2015, 55, 2269-2271.	0.6	12
77	First-principles Calculation of Effects of Carbon on Tetragonality and Magnetic Moment in Fe–C System. ISIJ International, 2015, 55, 2483-2491.	0.6	15
78	Positive and negative effects of hydrogen on tensile behavior in polycrystalline Fe–30Mn–(6 â^'x)Si–xAl austenitic alloys. Scripta Materialia, 2015, 105, 54-57.	2.6	38
79	Effect of deformation twin on toughness in magnesium binary alloys. Philosophical Magazine, 2015, 95, 2513-2526.	0.7	12
80	Microstructure Evolution Associated with a Superior Low-Cycle Fatigue Resistance of the Fe-30Mn-4Si-2Al Alloy. Metallurgical and Materials Transactions A: Physical Metallurgy and Materials Science, 2015, 46, 5103-5113.	1.1	24
81	Spatially and Kinetically Resolved Mapping of Hydrogen in a Twinning-Induced Plasticity Steel by Use of Scanning Kelvin Probe Force Microscopy. Journal of the Electrochemical Society, 2015, 162, C638-C647.	1.3	64
82	Designing Fe–Mn–Si alloys with improved low-cycle fatigue lives. Scripta Materialia, 2015, 99, 49-52.	2.6	129
83	Stress–strain behavior of ferrite and bainite with nano-precipitation in low carbon steels. Acta Materialia, 2015, 83, 383-396.	3.8	297
84	Deformation Twinning Behavior of Twinning-induced Plasticity Steels with Different Carbon Concentrations – Part 1: Atomic Force Microscopy and Electron Backscatter Diffraction Measurements. ISIJ International, 2015, 55, 1747-1753.	0.6	8
85	Hydrogen Embrittlement in Al-Added Twinning-Induced Plasticity Steels Evaluated by Tensile Tests during Hydrogen Charging. Tetsu-To-Hagane/Journal of the Iron and Steel Institute of Japan, 2014, 100, 662-667.	0.1	0
86	Deformation Twinning Behavior of Twinning-Induced Plasticity Steels with Different Carbon Concentrations. Tetsu-To-Hagane/Journal of the Iron and Steel Institute of Japan, 2014, 100, 1253-1260.	0.1	6
87	Deformation Twinning Behavior of Twinning-Induced Plasticity Steels with Different Carbon Concentrations. Tetsu-To-Hagane/Journal of the Iron and Steel Institute of Japan, 2014, 100, 1246-1252.	0.1	8
88	Effect of Initial Microstructure on Impact Toughness of 1200ÂMPa-Class High Strength Steel with Ultrafine Elongated Grain Structure. Metallurgical and Materials Transactions A: Physical Metallurgy and Materials Science, 2014, 45, 647-653.	1.1	7
89	Hydrogen-assisted decohesion and localized plasticity in dual-phase steel. Acta Materialia, 2014, 70, 174-187.	3.8	366
90	Crack propagation behaviour in magnesium binary alloys. Philosophical Magazine, 2014, 94, 3317-3330.	0.7	15

#	Article	IF	CITATIONS
91	Hydrogen embrittlement associated with strain localization in a precipitation-hardened Fe–Mn–Al–C light weight austenitic steel. International Journal of Hydrogen Energy, 2014, 39, 4634-4646.	3.8	170
92	Effects of Static and Dynamic Strain Aging on Hydrogen Embrittlement in TWIP Steels Containing Al. Tetsu-To-Hagane/Journal of the Iron and Steel Institute of Japan, 2014, 100, 1132-1139.	0.1	5
93	Ultrafine-Grain Structure Formation in an Al-Mg-Sc Alloy During Warm ECAP. Metallurgical and Materials Transactions A: Physical Metallurgy and Materials Science, 2013, 44, 1087-1100.	1.1	37
94	Application of orthogonally arranged FIB–SEM for precise microstructure analysis of materials. Journal of Alloys and Compounds, 2013, 577, S717-S721.	2.8	28
95	Hydrogen-assisted quasi-cleavage fracture in a single crystalline type 316 austenitic stainless steel. Corrosion Science, 2013, 75, 345-353.	3.0	85
96	Tempforming in medium-carbon low-alloy steel. Journal of Alloys and Compounds, 2013, 577, S538-S542.	2.8	28
97	Grain refinement effect on cryogenic tensile ductility in a Fe–Mn–C twinning-induced plasticity steel. Materials & Design, 2013, 49, 234-241.	5.1	61
98	Microstructure characteristic and its effect on mechanical and shape memory properties in a Fe–17Mn–8Si–0.3C alloy. Journal of Alloys and Compounds, 2013, 573, 15-19.	2.8	6
99	Studies of Evaluation of Hydrogen Embrittlement Property of High-Strength Steels with Consideration of the Effect of Atmospheric Corrosion. Metallurgical and Materials Transactions A: Physical Metallurgy and Materials Science, 2013, 44, 1290-1300.	1.1	43
100	Hydrogen-assisted failure in a twinning-induced plasticity steel studied under in situ hydrogen charging by electron channeling contrast imaging. Acta Materialia, 2013, 61, 4607-4618.	3.8	218
101	Toughening by the addition of phosphorus to a high-strength steel with ultrafine elongated grain structure. Philosophical Magazine Letters, 2013, 93, 109-115.	0.5	6
102	Effect of solute atoms on fracture toughness in dilute magnesium alloys. Philosophical Magazine, 2013, 93, 4582-4592.	0.7	39
103	Machinability Improvement and Its Mechanism in SUS304 Austenitic Stainless Steel by Precipitated Hexagonal Boron Nitride. ISIJ International, 2013, 53, 1841-1849.	0.6	5
104	TWIP Effect and Plastic Instability Condition in an Fe^ ^ndash;Mn^ ^ndash;C Austenitic Steel. ISIJ International, 2013, 53, 323-329.	0.6	67
105	Factors Affecting Static Strain Aging under Stress at Room Temperature in a Fe–Mn–C Twinning-induced Plasticity Steel. ISIJ International, 2013, 53, 1089-1096.	0.6	9
106	Effects of Static and Dynamic Strain Aging on Hydrogen Embrittlement in TWIP Steels Containing Al. ISIJ International, 2013, 53, 1268-1274.	0.6	24
107	Inverse grain size dependence of critical strain for serrated flow in a Fe–Mn–C twinning-induced plasticity steel. Philosophical Magazine Letters, 2012, 92, 145-152.	0.5	19
108	Hydrogen Embrittlement in Al-added Twinning-induced Plasticity Steels Evaluated by Tensile Tests during Hydrogen Charging. ISIJ International, 2012, 52, 2283-2287.	0.6	35

#	Article	IF	CITATIONS
109	Influence of Dislocation Separation on Dynamic Strain Aging in a Fe–Mn–C Austenitic Steel. Materials Transactions, 2012, 53, 546-552.	0.4	29
110	Effect of Dislocation Density on the Initiation of Plastic Deformation on Fe–C Steels. Materials Transactions, 2012, 53, 907-912.	0.4	30
111	Influence of Processing Regimes on Fine-Grained Microstructure Development in an Al–Mg–Sc Alloy by Hot Equal-Channel Angular Pressing. Materials Transactions, 2012, 53, 56-62.	0.4	13
112	Selective appearance of <i>ϵ</i> -martensitic transformation and dynamic strain aging in Fe–Mn–C austenitic steels. Philosophical Magazine, 2012, 92, 3051-3063.	0.7	28
113	Hydrogen embrittlement in a Fe–Mn–C ternary twinning-induced plasticity steel. Corrosion Science, 2012, 54, 1-4.	3.0	134
114	Effect of hydrogen content on the embrittlement in a Fe–Mn–C twinning-induced plasticity steel. Corrosion Science, 2012, 59, 277-281.	3.0	103
115	Effect of deformation temperature on tensile properties in a pre-cooled Fe–Mn–C austenitic steel. Materials Science & Engineering A: Structural Materials: Properties, Microstructure and Processing, 2012, 556, 331-336.	2.6	12
116	Premature Fracture Mechanism in an Fe-Mn-C Austenitic Steel. Metallurgical and Materials Transactions A: Physical Metallurgy and Materials Science, 2012, 43, 4063-4074.	1.1	52
117	Enhanced uniform elongation by pre-straining with deformation twinning in high-strength β-titanium alloys with an isothermal ω-phase. Philosophical Magazine Letters, 2012, 92, 726-732.	0.5	16
118	Quasi-cleavage Fracture along Annealing Twin Boundaries in a Fe–Mn–C Austenitic Steel. ISIJ International, 2012, 52, 161-163.	0.6	31
119	Hydrogen Embrittlement of a 1500-MPa Tensile Strength Level Steel with an Ultrafine Elongated Grain Structure. Metallurgical and Materials Transactions A: Physical Metallurgy and Materials Science, 2012, 43, 1670-1687.	1.1	61
120	Enhancement of Upper Shelf Energy through Delamination Fracture in 0.05Âpct P Doped High-Strength Steel. Metallurgical and Materials Transactions A: Physical Metallurgy and Materials Science, 2012, 43, 2453-2465.	1.1	27
121	Tensile deformation behavior of Fe–Mn–C TWIP steel with ultrafine elongated grain structure. Materials Letters, 2012, 75, 169-171.	1.3	69
122	Hydrogen-induced cracking at grain and twin boundaries in an Fe–Mn–C austenitic steel. Scripta Materialia, 2012, 66, 459-462.	2.6	168
123	Hydrogen-induced delayed fracture of a Fe–22Mn–0.6C steel pre-strained at different strain rates. Scripta Materialia, 2012, 66, 947-950.	2.6	50
124	Submicrocrystalline Structures and Tensile Behaviour of Stainless Steels Subjected to Large Strain Deformation and Subsequent Annealing. Advanced Materials Research, 2011, 409, 607-612.	0.3	2
125	Constant-load delayed fracture test of atmospherically corroded high strength steels. Applied Surface Science, 2011, 257, 8275-8281.	3.1	30
126	Hydrogen entry into Fe and high strength steels under simulated atmospheric corrosion. Electrochimica Acta, 2011, 56, 1799-1805.	2.6	77

#	Article	IF	CITATIONS
127	Work hardening associated with É≻martensitic transformation, deformation twinning and dynamic strain aging in Fe–17Mn–0.6C and Fe–17Mn–0.8C TWIP steels. Materials Science & Engineering A: Structural Materials: Properties, Microstructure and Processing, 2011, 528, 7310-7316.	2.6	185
128	Delamination Effect on Impact Properties of Ultrafine-Grained Low-Carbon Steel Processed by Warm Caliber Rolling. Metallurgical and Materials Transactions A: Physical Metallurgy and Materials Science, 2010, 41, 341-355.	1.1	141
129	Hydrogen embrittlement property of a 1700-MPa-class ultrahigh-strength tempered martensitic steel. Science and Technology of Advanced Materials, 2010, 11, 025005.	2.8	51
130	Evaluation of hydrogen entry into high strength steel under atmospheric corrosion. Corrosion Science, 2010, 52, 2758-2765.	3.0	115
131	Evaluation of susceptibility of high strength steels to delayed fracture by using cyclic corrosion test and slow strain rate test. Corrosion Science, 2010, 52, 1660-1667.	3.0	69
132	Evaluation of delayed fracture property of outdoor-exposed high strength AISI 4135 steels. Corrosion Science, 2010, 52, 3198-3204.	3.0	34
133	Delamination Toughening of Ultrafine Grain Structure Steels Processed through Tempforming at Elevated Temperatures. ISIJ International, 2010, 50, 152-161.	0.6	75
134	1104 Impact Properties of Low-Carbon Steel with Ultrafme Elongated Grain Structure. The Proceedings of the Computational Mechanics Conference, 2010, 2010.23, 125-126.	0.0	0
135	Evaluation of matrix strength in ultra-fine grained pure Al by nanoindentation. Journal of Materials Research, 2009, 24, 2917-2923.	1.2	14
136	Effects of severe plastic deformation on the corrosion behavior of aluminum alloys. Journal of Solid State Electrochemistry, 2009, 13, 277-282.	1.2	55
137	Development of Fine-Grained Structure Caused by Friction Stir Welding Process of a ZK60A Magnesium Alloy. Materials Transactions, 2009, 50, 610-617.	0.4	19
138	Inverse Temperature Dependence of Toughness in an Ultrafine Grain-Structure Steel. Science, 2008, 320, 1057-1060.	6.0	330
139	Slip System Partitioning as a Possible Mechanism for Ultrafine Grain Formation in Fe–3%Si Bicrystals. ISIJ International, 2008, 48, 1102-1106.	0.6	0
140	157 Improvement in Impact Toughness of a 1800 MPa-Class Low-Alloy Steel through the Use of Delamination. The Proceedings of the Computational Mechanics Conference, 2008, 2008.21, 700-701.	0.0	0
141	Effect of hydrogen on the fracture behavior of high strength steel during slow strain rate test. Corrosion Science, 2007, 49, 4081-4097.	3.0	336
142	Plasticity initiation and subsequent deformation behavior in the vicinity of single grain boundary investigated through nanoindentation technique. Journal of Materials Science, 2007, 42, 1728-1732.	1.7	58
143	Determination of the critical hydrogen concentration for delayed fracture of high strength steel by constant load test and numerical calculation. Corrosion Science, 2006, 48, 2189-2202.	3.0	129
144	A New Approach for Interpretation of Strengthening Mechanism of Martensitic Steel through Characterization of Local Deformation Behavior. Tetsu-To-Hagane/Journal of the Iron and Steel Institute of Japan, 2006, 92, 295-310.	0.1	8

#	Article	IF	CITATIONS
145	Microstructure effect on nanohardness distribution for medium-carbon martensitic steel. Science in China Series D: Earth Sciences, 2006, 49, 10-19.	0.9	7
146	Indentation-Induced Deformation Behavior in Martensitic Steel Observed through In Situ Nanoindentation in a Transmission Electron Microscopy. Materials Science Forum, 2006, 503-504, 239-244.	0.3	3
147	Hydrogen Entry in Crevice Region: Evaluation by Hydrogen Permeation Technique. ISIJ International, 2006, 46, 1081-1085.	0.6	8
148	Nanoindentation-Induced Deformation Behavior in the Vicinity of Single Grain Boundary of Interstitial-Free Steel. Materials Transactions, 2005, 46, 2026-2029.	0.4	82
149	Evaluation of Grain Boundary Effect on Strength of Fe–C Low Alloy Martensitic Steels by Nanoindentation Technique. Materials Transactions, 2005, 46, 1301-1305.	0.4	17
150	Hydrogen degradation of a boron-bearing steel with 1050 and 1300MPa strength levels. Scripta Materialia, 2005, 52, 403-408.	2.6	130
151	Response of hydrogen trapping capability to microstructural change in tempered Fe–0.2C martensite. Scripta Materialia, 2005, 52, 467-472.	2.6	89
152	Effect of hydrogen and stress concentration on the notch tensile strength of AISI 4135 steel. Materials Science & Engineering A: Structural Materials: Properties, Microstructure and Processing, 2005, 398, 37-46.	2.6	226
153	Light Pre-deformation induced misorientation of grain boundary bcc-precipitates from the Kurdjumov-Sacks relationship in a Niâ°Cr alloy. Metals and Materials International, 2005, 11, 341-349.	1.8	4
154	Evaluation of Grain Boundary Effect on the Strength of Fe-C Martensitic Steels through Nanoindentation Technique. Materials Science Forum, 2005, 475-479, 4113-4116.	0.3	5
155	High-resolution transmission electron microscopy study of crystallography and morphology of TiC precipitates in tempered steel. Philosophical Magazine, 2004, 84, 1735-1751.	0.7	68
156	Effect of Nano-Sized Oxides on Annealing Behaviour of Ultrafine Grained Steels. Materials Transactions, 2004, 45, 2252-2258.	0.4	11
157	Microstructure Evolution in Ferritic Stainless Steels during Large Strain Deformation. Materials Transactions, 2004, 45, 2812-2821.	0.4	46
158	Hydrogen Trapping in Quenched and Tempered 0.42C-0.30Ti Steel Containing Bimodally Dispersed TiC Particles. ISIJ International, 2003, 43, 539-547.	0.6	109
159	Low-and High-cycle Fatigue Properties of Ultrafine-grained Low Carbon Steels. Tetsu-To-Hagane/Journal of the Iron and Steel Institute of Japan, 2003, 89, 726-733.	0.1	23
160	Relationship between Precipitation of Nano-Sized TiC and Hydrogen Absorption Property in a Ti-Bearing High-trength Steel. Materia Japan, 2003, 42, 884-884.	0.1	0
161	OS06W0420 Nanoindentation technique as a probe for characteristic deformation size. The Abstracts of ATEM International Conference on Advanced Technology in Experimental Mechanics Asian Conference on Experimental Mechanics, 2003, 2003.2, _OS06W0420OS06W0420.	0.0	0
162	Microstructural Analyses of Grain Boundary Carbides of Tempered Martensite in Medium-Carbon Steel by Atomic Force Microscopy. Materials Transactions, 2002, 43, 1758-1766.	0.4	14

#	Article	IF	CITATIONS
163	Microstructural Analyses of Modified-Ausformed Medium-Carbon Steel with High Resistance to Hydrogen Embrittlement by Atomic Force Microscopy. Nippon Kinzoku Gakkaishi/Journal of the Japan Institute of Metals, 2002, 66, 745-753.	0.2	28
164	Preface to the Special Issue on "Advanced Structural Steels― ISIJ International, 2002, 42, 1325-1325.	0.6	5
165	Determination Method of Weibull Shape Parameter for Evaluation of the Hydrogen Embrittlement Susceptibility of High Strength Steel. Nippon Kinzoku Gakkaishi/Journal of the Japan Institute of Metals, 2001, 65, 1082-1090.	0.2	8
166	Observations of Prior Austenite Grain Boundaries and Carbides in the Same Area of Tempered Martensite in Medium-Carbon Steel by Atomic Force Microscopy. Nippon Kinzoku Gakkaishi/Journal of the Japan Institute of Metals, 2001, 65, 734-741.	0.2	10
167	Evaluation of Hydrogen Embrittlement Susceptibility of High Strength Steel by the Weibull Stress. Nippon Kinzoku Gakkaishi/Journal of the Japan Institute of Metals, 2001, 65, 1073-1081.	0.2	19
168	Preface to the Special Issue on "Advances in Physical Metallurgy and Processing of Steels". ISIJ International, 2001, 41, 519-519.	0.6	0
169	The Morphology of Microstructure Composed of Lath Martensites in Steels. Transactions of the Iron and Steel Institute of Japan, 1980, 20, 207-214.	0.2	161
170	Recrystallization Mechanisms in Severely Deformed Dual-Phase Stainless Steel. Materials Science Forum, 0, 638-642, 1905-1910.	0.3	8
171	Role of Delamination Fracture for Enhanced Impact Toughness in 0.05 %P Doped High Strength Steel with Ultrafine Elongated Grain Structure. Advanced Materials Research, 0, 409, 231-236.	0.3	1
172	Dynamic Recrystallization Mechanisms Operating under Different Processing Conditions. Materials Science Forum, 0, 706-709, 2704-2709.	0.3	5
173	Low-Cycle Fatigue Behavior and Microstructural Evolution of the Fe–30Mn–4Si–2Al Alloy. Materials	0.3	2